scientific reports

Check for updates

OPEN

Assessment of dermal fiber changes associated with age ethnicity and cosmetic product use by LC-OCT and automated 3D segmentation

Kamilia Kemel[1]✉, Randa Jdid[1], Julie Latreille[1], Oriane Tarby[2], Lucas Gandel[3], Severine Ponsero[4], Nada André[1], Gabriel Cazorla[1] & Youcef Ben Khalifa[1]

This work presents a novel, non-invasive method that combines high-resolution 3D Line-field Confocal Optical Coherence Tomography (LC-OCT) images with an advanced, in-house developed automated 3D segmentation algorithm to quantitatively analyze dermal fiber characteristics in vivo. This approach marks the first in-depth investigation of dermal fibers, enabling precise characterization of age-related changes, ethnic differences, and the effects of anti-aging skincare products on the cheekbone region of Caucasian and Asian women. Our algorithm accurately extracts fiber metrics, revealing that aging correlates with shorter fiber length and increased anisotropy. Although Asians exhibited a denser fiber network than Caucasians, both ethnicities showed comparable mean fiber lengths and anisotropy. Furthermore, anti-aging skincare treatments significantly enhanced fiber length, node count, and network density while reducing anisotropy over one and three months. This innovative integration of cutting-edge imaging and algorithmic analysis provides valuable insights for cosmetic applications and paves the way for future non-invasive dermatological research.

Keywords Dermal fibers, Automated segmentation, Skin aging, Anti-aging skin care products, Line field confocal optical coherence tomography

Skin imaging plays a central role in understanding tissue microstructure, driving the development of various non-invasive techniques over recent decades to study changes in dermal fiber networks. These methods include ultrasonic microscopy[1], second harmonic generation (SHG) microscopy[2], multiphoton imaging (MPM)[3,4], fluorescence photography (FP) and fluorescence spectroscopy (FS)[5], reflectance confocal microscopy (RCM) and optical coherence tomography (OCT)[6,7]. However, some limitations inherent to these techniques hinder a comprehensive analysis of changes in dermal fibers properties. MPM has a significantly slower scanning rate than OCT and RCM, and both MPM and RCM have limited penetration depth compared with OCT[4,8]. The resolution of RCM is in the micrometer range and the depth of penetration is limited to around 200 µm, whereas the resolution of conventional OCT is 3–15 µm and the depth of 1 mm which is not sufficient for cell imaging[9]. Fluorescence-based methods are useful for global evaluation but are limited in spatial resolution[5]. Line-field Confocal Optical Coherence Tomography (LC-OCT) is an innovative non-invasive imaging technique that combines the principles and advantages of RCM and OCT[10–12]. This technology allows the generation of vertical and horizontal sections as well as three-dimensional (3D) images of epidermis and the superficial dermis with high resolution similar to histology (~1 µm) and a penetration depth of 400–500 µm[10–13].

In fact, the skin consists of connective tissue, primarily composed of collagen and elastin fibers embedded in a host gel-like structure. Collagen fibers are a major component of the dermis, accounting for around 60–80% of the dry weight of skin, and provide tensile strength, giving the skin its firmness and structure[14,15]. Elastin fibers comprise 4% of the fat-free dry mass, providing elasticity to allow the skin to stretch and return to its original shape after deformation[14,15]. Together, collagen and elastin form a network that maintains the skin's structural integrity, elasticity, and resilience[16]. With aging, the dermis experiences compositional and organizational

[1]IRD Chanel Fragrance & Beauty, 8 Rue du Cheval Blanc, Pantin Cedex 93694, France. [2]IT&M STATS, Boulogne-Billancourt, France. [3]Kitware Europe, Lyon, France. [4]DERMATECH, Lyon, France. ✉email: kamilia.kemel@chanel.com

changes that lead to dermal fibers alteration and disruption of the structural integrity of the extracellular matrix (ECM)[17,18]. This process is primarily driven by a decrease of collagen and elastin dermis contents and an increase of collagen cross-linking[2,19,20]. Such structural transformations weaken the mechanical properties of the tissue, leading to increased fragility[21] and the formation of wrinkles[22]. Skin microstructures also vary by ethnicity, however, comparative studies examining these differences from histological and structural perspectives remain limited in the literature[23].

Previous studies reveal that Asian skin have higher levels of melanin and collagen compared to Caucasian skin[24]. They seem to possess larger fibroblasts and denser structure of collagen bundles compared with other ethnicities[25]. Caucasian skin, in contrast, is marked by a thinner and less cohesive stratum corneum, reduced extensibility, collagen loss, and disorganized elastic fibers in the dermis, contributing to its fragility, earlier aging, and more pronounced wrinkles and sagging compared to other skin types[26,27]. Understanding the structural changes associated with dermis aging processes is crucial for developing effective cosmetic products. While a wide range of skincare products has been created to maintain a youthful appearance[20,28], the precise molecular mechanisms underlying their ingredients' actions remain unclear. This underscores the need for detailed in vivo analysis of dermal fiber structures and their response to these active compounds. In this context, LC-OCT coupled with Artificial Intelligence (AI)-based segmentation algorithms, offer detailed insights into skin structure and tissue evolution of healthy skin[29,30] as well as dark spot morphology[31], identification of facial skin ageing biomarkers[32] and assessment of skin care product efficacy[31,33]. These algorithms enable to compute various metrics, including stratum corneum (SC) and viable epidermal (VE) thickness[11,23], dermal-epidermal junction (DEJ) undulation[31] and nuclei size, shape and density of keratinocyte network[34].

In this study, we developed a new algorithm for automated 3D segmentation of dermal fibers from LC-OCT images. This was visually validated by performing a slice-by-slice comparison of the segmented and original images in a set of representative cases. This algorithm extracts relevant information and calculates, for the first time, various metrics, including the number and mean length of fibers, the number of nodes, the anisotropy score, and the density of the fiber network. To our knowledge, only one study conducted by Ayadh M., et al.[35] has focused on the density and diameter of fibers in the papillary dermis using LC-OCT, limited to 2D segmentation from horizontal images calculating only fibers density and diameter metrics[35]. Working in 3D provides more comprehensive information about the spatial organization and structure of fibers within the volume than is accessible through 2D analysis alone.

The present study aims to explore for the first time the generated metrics to analyze the impact of aging, ethnicity (Asian and Caucasian), and the use of a combined skincare routine (serum and cream) on the characteristics of the facial dermal fiber network.

Results

The developed methodology enables the automatic 3D segmentation of dermal fibers, facilitating the structural analysis of skin tissues. To demonstrate the relevance of this approach, two categories of images were selected: young individual (30 years old) and aged individual (63 years old with a particular case where fibers are oriented in parallel), as shown in Figure S1. To ensure a fair and consistent comparison, all measurements in this study were performed on the same anatomical site, the cheekbone, for all participants.

The results clearly highlight these two structural patterns. This clear distinction supports the algorithm's ability to capture relevant microstructural differences. The effectiveness of this approach is further supported by the associated metrics (the number and mean length of fibers, the number of nodes, the anisotropy score, and the density of the fiber network), which provide a precise characterization of fiber morphology and organization (cf. image processing in Methods section). Given the performance of the developed methodology, we applied it to images from two clinical studies conducted to investigate the effects of age, ethnicity, and cosmetic skincare products.

Study 1: impact of aging and ethnicity on dermal fibers

Figures 1 and 2 illustrate differences in the measured metrics of the fiber network based on age and ethnicity. The statistical analysis of these differences is presented in Table 1. The number of fibers was not statistically different between both studied age groups, while their mean length decreased significantly with age ($P=0.0310$). These observations hold true for both connected (with nodes) and isolated (without nodes) fibers, as well as when analyzed together (Fig. 1A, B; Table 1). The number of the nodes and the density were not significantly different, while the anisotropy score increased statistically with age ($P=0.0438$) (Fig. 1C–E; Table 1).

Schematic representations of these skin age characteristics are illustrated in Figure S2. The comparison between the two ethnic groups revealed that the number of fibers was significantly higher in the Asian group compared to the Caucasian group ($P=0.0009$), while their mean length was not significantly different. This observation was consistent for both connected and isolated fibers, as well as when analyzed together (Fig. 2A, B; Table 1). The number of nodes and density were significantly higher ($P=0.0139$, $P=0.0060$ respectively) in the Asian group than in the Caucasian group (Fig. 2C, D; Table 1). Schematic representations of these ethnic differences are shown in Figure S3. The anisotropy score was not statistically different between the Asian and Caucasian groups (Fig. 2E; Table 1).

Study 2: effect of an anti-aging skincare products application

We assessed the effects of an anti-aging skincare product (the core ingredients is botanical alfalfa concentrate) on the dermal fibers of 31 Caucasian women after one month (t_1) and three months (t_3) of application (Fig. 3). The statistical analysis of the effect over each period is presented in Table 1. Compared to baseline (t_0), the number of connected fibers was significantly decreased after one month ($P=0.012$) of application, while the number of isolated fibers was not significantly different. The total number of the two types of fibers decreased

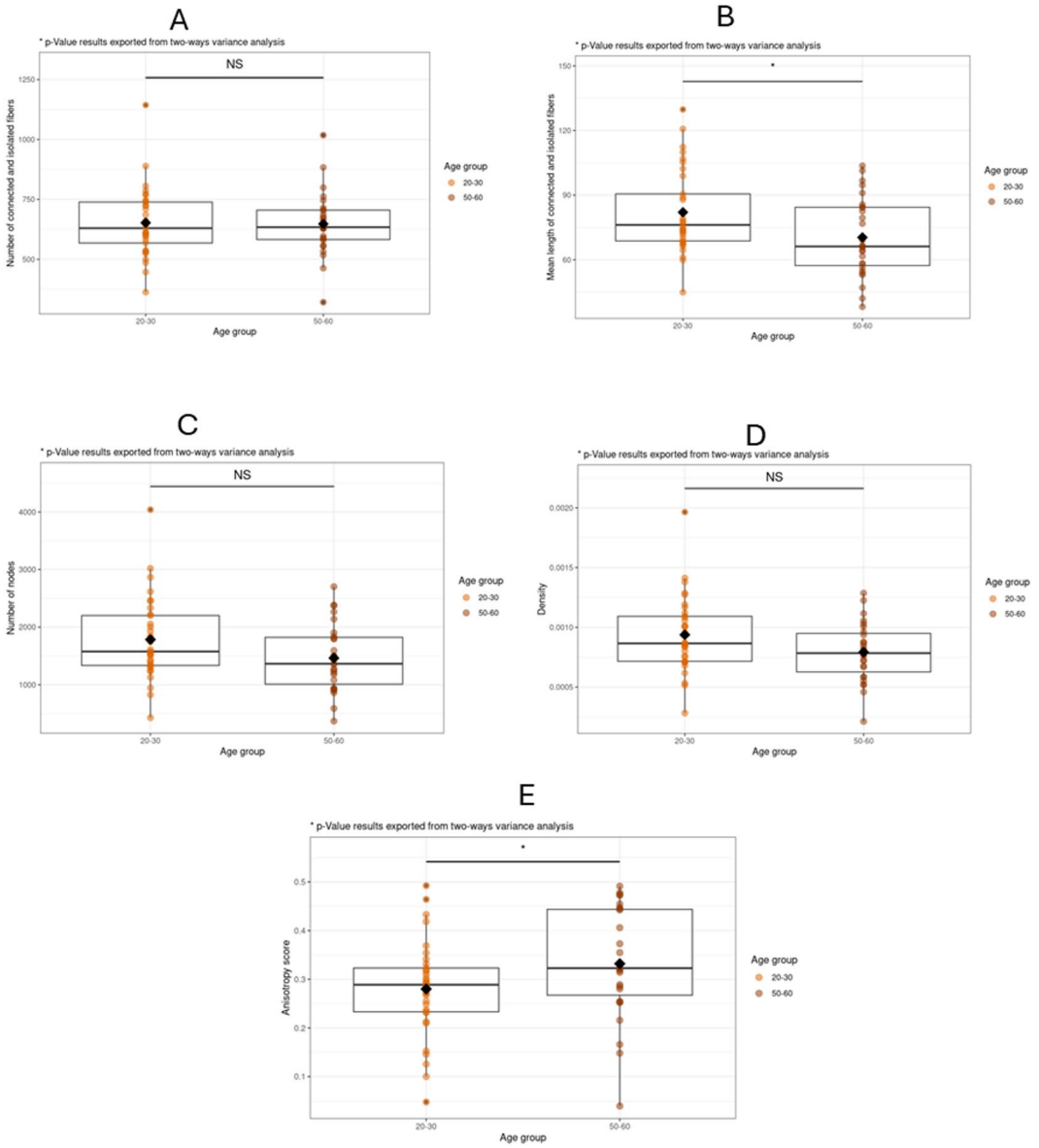

Fig. 1. Variation in dermal fiber metrics according to age. Boxplot illustrating. The changes in number (**A**) and mean length (**B**) of connected and isolated dermal fibers across two age groups: [20–30] 33 women aged between 20 and 30 years old; [50–60] 27 women aged between 50 and 60 years old. The changes in number of nodes (**C**), density (**D**) and anisotropy score (**E**) for fiber network across two age groups: [20–30] 33 women aged between 20 and 30 years old; [50–60] 27 women aged between 50 and 60 years old.

but not significantly (Fig. 3A; Table 1). The mean length of the connected fibers exhibited a significant increase ($P = 0.006$), while the mean length of the isolated fibers exhibited a significant decrease ($P = 0.000$).The significant increase in mean length of total fibers (Fig. 3B; Table 1) despite the decrease in isolated fibers length, may be explained by the predominant influence of connected fibers when analyzed together.

The number of nodes exhibited a notable increase ($P = 0.009$), and the density tended to rise. In contrast, the anisotropy score exhibited a significant reduction ($P = 0.004$). These results were consistent with the second point of measurement when comparing the baseline (t_0) and three months later (t_3). The sole distinction between the two periods was that the density exhibited a marked increase ($P = 0.007$) after three months, whereas it exhibited a trend to increase ($P = 0.072$) after one month (Fig. 3C–E; Table 1). Figure S4 illustrates the schematic representations of dermal fiber changes following one month of cosmetic product application.

Discussion

Using non-invasive LC-OCT 3D imaging combined with our advanced automated 3D segmentation algorithms, we quantified fiber number, mean length, node count, anisotropy, and network density. Unlike Ayadh M. et al.[35] who analyzed only fiber density and diameter in LC-OCT 2D imaging, our 3D approach provides a more complete characterization of fiber spatial organization and structure.

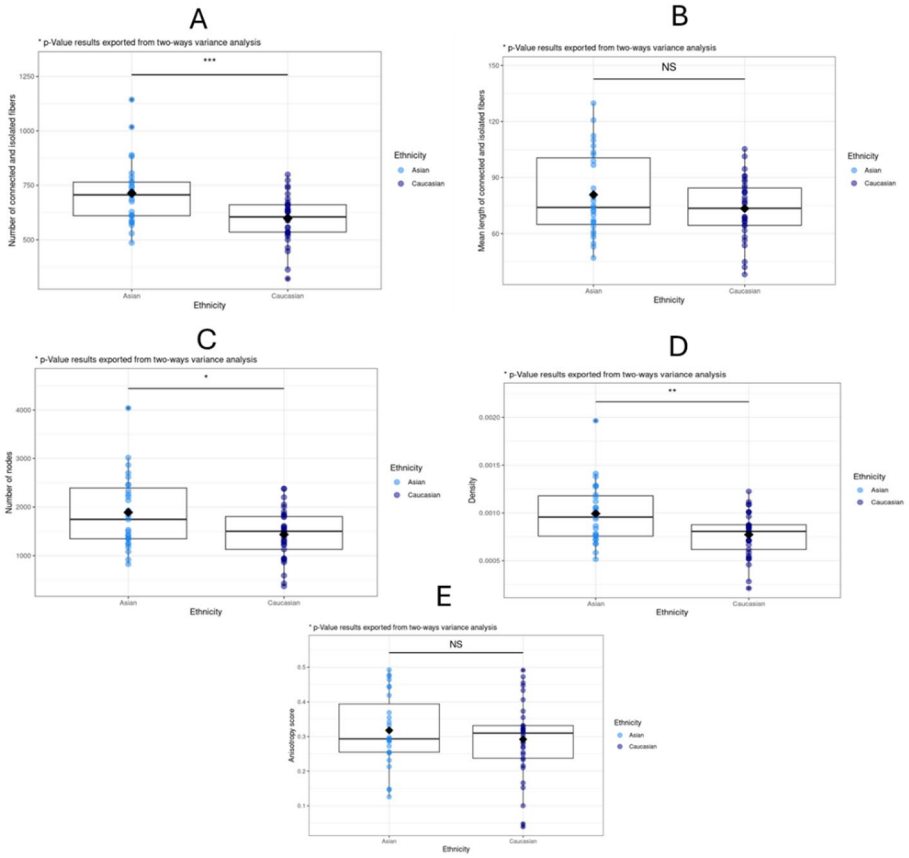

Fig. 2. Variation in dermal fiber metrics according to age and ethnicity. Boxplot illustrating: the changes in number (**A**) and mean length (**B**) of connected and isolated dermal fibers across two ethnic groups: 27 Asian women and 33 Caucasian women. The changes in number of nodes (**C**), density (**D**) and anisotropy score (**E**) for fiber network across two ethnic groups: 27 Asian women and 33 Caucasian women.

We have conducted an extensive and detailed analysis to explore the effects of various factors such as age, ethnicity and the use of skin care products on the properties of dermal fibers. Although these results should be interpreted with caution, due to multiple tests on numerous metrics, this approach allows for precise visualization and quantification of the structural changes in the dermal extracellular matrix, offering valuable insights into how these factors contribute to the degradation or modification of dermal fibers over time across different populations.

Dermal fibers are one of the key components of the dermis, capable of undergoing significant structural and functional changes due to different factors such as aging, chronic sun exposure, environmental influences and lifestyle choices[23,36]. Our study demonstrated that aging significantly impacts the mean length of fibers. The reduction in fiber length with age could be explained by fibers fragmentation/degradation as reported in the literature[20,37,38]. Histology and multiphoton imaging revealed that in old cheek skin, higher amounts of elastotic tissue could be observed while collagen almost completely fragmented and disappeared[37]. Fligiel et al.[39] employed biochemical and ultrastructural approaches to demonstrate that photodamaged skin exhibited extensive collagen fragmentation and clumping, while sun-protected aged skin exhibited similar damage, but with less extensive damage in individuals aged 80 years or older. In contrast, sun-protected young (18–29 years of age) skin exhibited minimal damage[39]. This fragmentation process is attributed to increased expression of matrix metalloproteinases (MMPs) and inhibition of TGF-β signaling, caused by reactive oxygen species (ROS) generated through aging and UV radiation. These mechanisms result in collagen degradation and decreased collagen synthesis[16,40]. Experiments on sun-protected human skin added to purified human MMP-1 in culture media result in similar collagen fragmentation and disordered fibril architectural changes within the dermis as in aged skin[17]. Furthermore, elastic fibers, which are thin and unbranched in youthful skin, progressively develop a beaded appearance in aged skin, along with the loss of terminal fibrils that extend into the epidermis[19].

We also observed that the number of fibers, the number of nodes, and the density of the fiber network did not significantly differ with age, suggesting that the structural framework of fibers may still be preserved. It was anticipated that these parameters would decline with age as reported in the literrature[38]; however, the findings of our study do not confirm this hypothesis. The most probable explanation for this discrepancy is that the age range of older individuals in this study was between 50 and 60 years old, which is not sufficiently advanced to demonstrate a significant decline. Indeed, Marcos-Garces et al.[41] demonstrated that collagen density in the reticular dermis peaks at birth (81%) but declines steadily, stabilizing between ages 40 and 60 (68% at 50

Metrics	Clinical study no. 1: Skin aging and comparison between two ethnic groups		Clinical study no. 2: Effect of an anti-aging product on fiber dermis	
	Age effect Y (*N* = 33) vs. O (*N* = 27)	**Ethnicity effect A (*N* = 27) vs. C (*N* = 33)**	**t_0 vs. t_1 (*N* = 31)**	**t_0 vs. t_3 (*N* = 24)**
Number of connected and isolated fibers	Y = 652 ± 144 O = 648 ± 133	A = 714 ± 147 C = 598 ± 107	t_0 = 412 ± 51 t_1 = 399 ± 69	t_0 = 421 ± 53 t_3 = 407 ± 47
	Two-ways Anova F(1,57) = 0.133, *p* = 0.717 (NS)	*Two-ways Anova* F(1,57) = 12.362, p = **0.001 (S)**	*Paired t-test* t(30) = 1.069, *p* = 0.294 (NS)	*Paired t-test* t(23) = 1.047, *p* = 0.306 (NS)
Number of connected fibers	Y = 151 ± 36 O = 147 ± 35	*A = 165 ± 39* *C = 137 ± 26*	t_0 = 97 [18] t_1 = 87 [35]	t_0 = 97 [28] t_3 = 89 [25]
	Two-ways Anova F(1,57) = 0.004, *p* = 0.952 (NS)	*Two-ways Anova* *F(1,57) = 11.240,* *p = 0.001 (S)*	*Wilcoxon signed rank test* z(30) = 375, p = **0.012 (S)**	*Wilcoxon signed rank test* z(23) = 248, p = **0.005 (S)**
Number of isolated fibers	Y = 501 ± 111 O = 500 ± 102	A = 549 ± 111 C = 462 ± 85	t_0 = 311 ± 37 t_1 = 310 ± 48	t_0 = 316 ± 38 t_3 = 317 ± 35
	Two-ways Anova F(1,57) = 0.204, *p* = 0.653 (NS)	*Two-ways Anova* F(1,57) = 11.789, p = **0.001 (S)**	*Paired t-test* t(30) = 0.155, *p* = 0.878 (NS)	*Paired t-test* t(23) = -0.071, *p* = 0.944 (NS)
Length of connected and isolated fibers	Y = 82 ± 19 O = 70 ± 18	A = 81 ± 23 C = 73 ± 16	t_0 = 121 ± 32 t_1 = 138 ± 40	t_0 = 115 ± 29 t_3 = 133 ± 31
	Two-ways Anova F(1,57) = 4.890, p = **0.031 (S)**	*Two-ways Anova* F(1,57) = 1.413, *p* = 0.240 (NS)	*Paired t-test* t(30) = -2.089, p = **0.045 (S)**	*Paired t-test* t(23) = -2.639, p = **0.015 (S)**
Length of connected fibers	Y = 310 ± 98 O = 262 ± 82	A = 308 ± 115 C = 273 ± 69	t_0 = 462 ± 151 t_1 = 596 ± 227	t_0 = 431 ± 134 t_3 = 580 ± 186
	Two-ways Anova F(1,57) = 3.346, *p* = 0.073 (T)	*Two-ways Anova* F(1,57) = 1.417, *p* = 0.239 (NS)	*Paired t-test* t(30) = -2.966, p = **0.006 (S)**	*Paired t-test* t(23) = -3.717, p = **0.001 (S)**
Length of isolated fibers	Y = 14.62 ± 0.63 O = 14.28 ± 0.72	A = 14.55 ± 0.72 C = 14.40 ± 0.66	t_0 = 13.87 ± 0.76 t_1 = 13.36 ± 0.60	t_0 = 14.01 ± 0.80 t_3 = 13.37 ± 0.71
	Two-ways Anova F(1,57) = 3.408, *p* = 0.070 (T)	*Two-ways Anova* F(1,57) = 0.388, *p* = 0.536 (NS)	*Paired t-test* t(30) = 4.051, p = **0.000 (S)**	*Paired t-test* t(23) = 3.155, p = **0.004 (S)**
Number of nodes	Y = 1785 ± 710 O = 1463 ± 581	A = 1890 ± 757 C = 1435 ± 515	t_0 = 1804 ± 494 t_1 = 2116 ± 555	t_0 = 1717 ± 462 t_3 = 2124 ± 497
	Two-ways Anova F(1,57) = 2.524, *p* = 0.118 (NS)	*Two-ways Anova* F(1,57) = 6.445, p = **0.014 (S)**	*Paired t-test* t(30) = -2.783, p = **0.009 (S)**	*Paired t-test* t(23) = -4.095, p = **0.000 (S)**
Density	Y = 0.00094 ± 0.00032 O = 0.00079 ± 0.00024	A = 0.00099 ± 0.00032 C = 0.00077 ± 0.00023	t_0= 0.00190 ± 0.00037 t_1=0.00206 ± 0.00038	t_0 = 0.00185 ± 0.00035 t_3=0.00207 ± 0.00038
	Two-ways Anova F(1,57) = 2.662, *p* = 0.108 (NS)	*Two-ways Anova* F(1,57) = 8.134, p = **0.006 (S)**	*Paired t-test* t(30) = -1.861, *p* = 0.072 (T)	*Paired t-test* t(23) = -2.959, p = **0.007 (S)**
Anisotropy score	Y = 0.280 ± 0.098 O = 0.332 ± 0.113	A = 0.318 ± 0.104 C = 0.292 ± 0.111	t_0 = 0.554 ± 0.096 t_1 = 0.499 ± 0.119	t_0 = 0.570 ± 0.095 t_3 = 0.506 ± 0.098
	Two-ways Anova F(1,57) = 4.250, p = **0.044 (S)**	*Two-ways Anova* F(1,57) = 1.526, *p* = 0.222 (NS)	*Paired t-test* t(30) = 3.076, p = **0.004 (S)**	*Paired t-test* t(23) = 3.324, p = **0.003 (S)**

Table 1. Statistical analysis results for the two studies. p: p-value; S: significant ($p < 0.05$). NS: not significant ($p > 0.10$). T: Trend ($0.05 < p < 0.10$); Y: Young; O: old; A: Asian; C: Caucasian. The measurements of anti-aging efficacy were taken at three timepoints: t_0 (before starting of the care routine), t_1 (after one month) and t_3 (after three months). Df : degree of freedom. Two -ways ANOVA : F(between groups df, within groups df) = [F-value]. T-test : t(df) = [Student-value]. Wilcoxon test : z(df) = [z-value].

years) before decreasing further with skin aging, reaching 58% by 100 years. It can therefore be understood that the aging process begins with fiber fragmentation, then later with advanced fragmentation, the fiber network would have a loss of connectivity[2] and a decrease in density[21]. Future research should focus on understanding the behavior of skin aging after 60 years old. The observed increase in the anisotropy score, illustrated in the schematic representation of skin aging in the supplementary figure of this study, indicates a change in the directional organization of the fibers. By aging, dermal fibers tend to orient themselves in a preferred direction. In their study, Nguyen et al.[18] employed polarized-FTIR imaging to examine the morphological alterations in dermal collagen, during chronological aging. They found that type I collagen fibers undergo reorientation, becoming parallel to the skin surface with age. This reorientation may be linked to a weakening of interactions between water and collagen with age[42,43]. Another explanation comes from polarization-resolved second-harmonic generation (SHG) microscopy, which was used to examine the orientation of dermal collagen fibers in photoaged UVB-exposed skin. The findings revealed that, in unexposed skin, dermal collagen fibers typically align along the body's meridian line. However, UVB exposure degrades collagen, prompting fibroblasts to realign and produce new collagen fibers in a horizontal direction. This shift in fibroblast orientation leads to a change in collagen alignment from vertical to horizontal[44,45].

The effect of ethnicity on dermal fibers is a crucial topic for understanding variations in skin aging across different populations. Our comparison between Asian and Caucasian groups revealed notable differences in

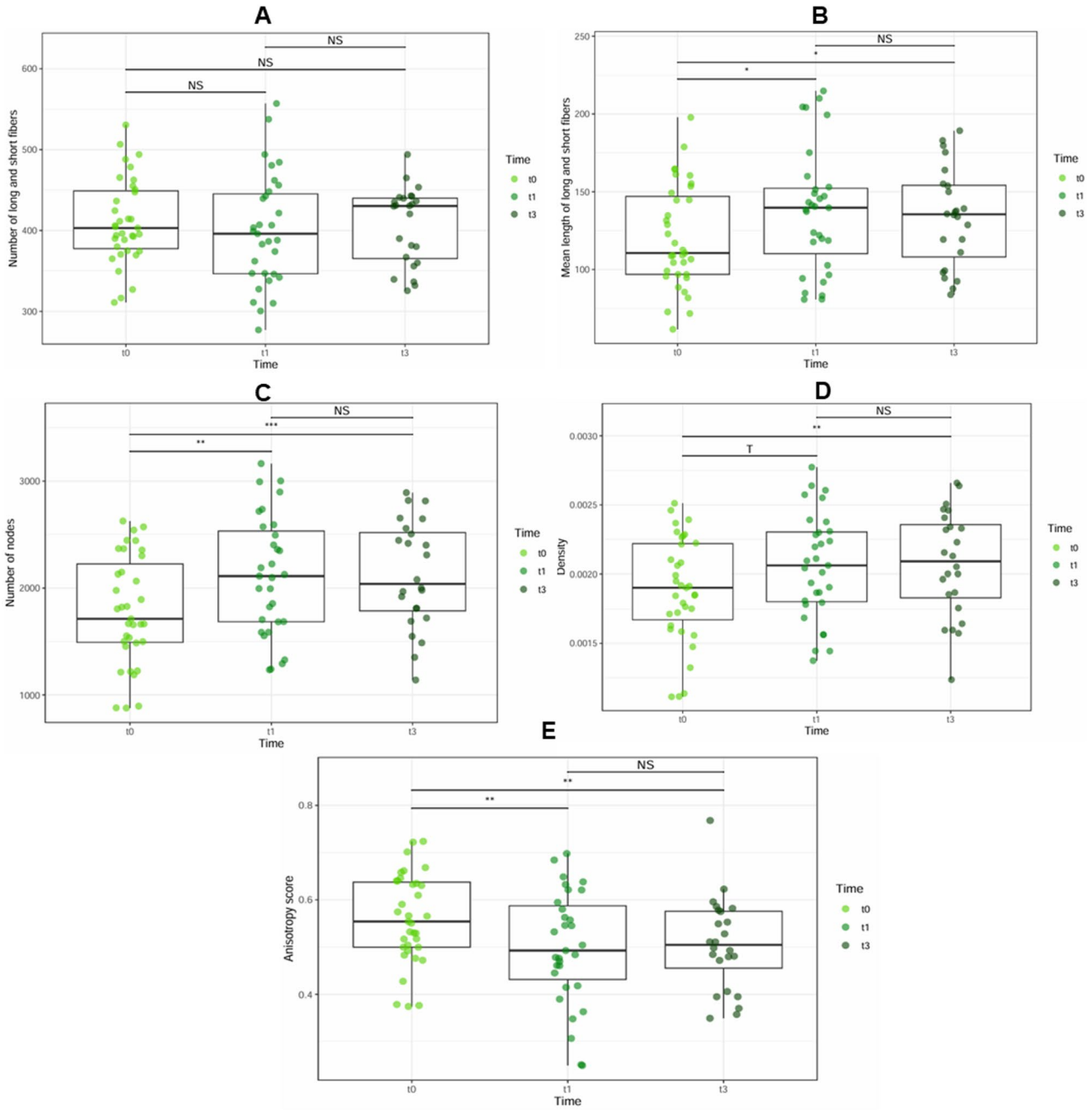

Fig. 3. Effectiveness of anti-aging products over a three-month period. Boxplot depicting: the number (**A**) and mean length (**B**) of dermal fibers at three timepoints: before starting a care routine (t_0) and after one (t_1) and three months (t_3) of using skincare products, 31 Caucasian women aged between 30 and 65 years old were evaluated. The number of nodes (**C**), density (**D**) and anisotropy score (**E**) of dermal fibers at three timepoints: before starting a care routine (t_0) and after one (t_1) and three months (t_3) of using skincare products, 31 Caucasian women aged between 30 and 65 years old were evaluated.

dermal fiber characteristics. Asians exhibited a higher number of dermal fibers and connectivity, and greater density compared to Caucasians, as demonstrated by the schematic representation of ethnic differences in this study. These observations are consistent with literature[46] and can be attributed to two primary factors. The first point to be considered is the amount of melanin present in different ethnic groups. Individuals of Asian and Black ethnicities possess greater quantities of melanin than those of Caucasian ethnicity. This may confer a more protective effect on the Asian dermis[25,27]. The second point is that Dark (Black and Asian) skin have a thicker and more compact dermis due to the presence of more fibroblasts than white skin[25,27,47]. Moreover, it was demonstrated that people with colored skin experience less UV-dependent elastin loss compared to Caucasians, and have elevated TGF-β1 signaling, which contributes to greater elastin production[48]. In addition, others factors, such as genetics and lifestyle, are well known to contribute to the ageing process. Genetic differences in

skin structure also mean that the signs of photoaging in Asian skin differ from those in white skin[25,27]. Despite these differences in number and density, the mean length of the fibers and the anisotropy score did not differ significantly between the groups. Similarly, Girardeau et al.[49] using microscopy, reported a difference in the density of collagen fibers while no differences in the organization of elastic and collagen fibers between Caucasian and African mammary skin biopsies. In addition, they also reported considerable variability in fiber length[49]. The second study evaluating the effect of anti-aging skin care products, showed promising results in modifying the structural properties of dermal fibers. After one month of application, the number of connected fibers decreased, and their mean length and number of nodes increased. This could suggest the development of new connections between these fibers, possibly in the form of bridges. The number of isolated fibers was not significantly different, yet their mean length decreased. With the increased density of the fiber network, it is plausible that the isolated fibers were associated with the connected ones, while at the same time, new fibers, more isolated than the originals, were synthesized. This would explain why the number of isolated fibers remained constant while their mean length decreased. Indeed, the active ingredient utilized in the formulation of anti-aging skincare products has retinol-like activity. The literature mentioned that retinoids stimulates the activity of fibroblasts to synthesize collagen fibers, enhances production of elastin fibers, inhibits matrix metalloproteinases (MMPs) and enhances synthesis of tissue inhibitors of metalloproteinases (TIMPs)[50–52]. These biological actions of retinoids provide a mechanistic explanation for the structural changes observed in our study, including increased fiber density and the formation of new connections (node) within the dermal network due to the fibroblasts activity. The inhibition of MMPs and enhancement of TIMPs reduces fiber degradation, thereby supporting the observed increase in fiber length and density. The reduction in the anisotropy score indicated a reorganization of the fiber network due to the establishment of new connections. This implied that fibers tend to orient themselves in various directions in comparison to their initial state. Humbert PG et al.[53] reported that after topical application of 5% vitamin C cream there was a significant increase in skin microrelief density, shown by a decrease in the anisotropy index and a reduction in deep furrows. The skin relief parameters were determined by the authors using silicone rubber. Goberdhan et al.[6] utilized RCM and Dynamic-OCT to study the impact of a topical retinol on facial photodamage. Their findings indicated that improved collagen fiber quality was accompanied by a significant increase in attenuation coefficient and collagen density, suggesting more compact and organized collagen. It is noteworthy that the improvements in the structural properties of dermal fibers observed in our study were sustained for a period of three months, not only indicating the long-lasting effectiveness of the products but also providing a more comprehensive understanding of their impact. Previous studies reported that OCT were mainly qualitative, allows image acquisition in two dimensional cross sections. It makes it possible to differentiate the three layers of the skin with good resolution: the stratum corneum, the viable epidermis and the dermis, but the depth of penetration remains very limited[35]. Whereas our research employed advanced imaging techniques, such as LC-OCT 3D imaging, which allowed for a more precise and detailed analysis of dermal fiber properties. Additionally, our study considered a broader range of parameters, including anisotropy score and fiber length, which provided deeper insights into the structural changes induced by the treatments. These methodological advancements, combined with the sustained results observed, offer a more robust evaluation of the effectiveness of anti-aging products.

In this study, we have developed a new automatic algorithm for dermal fiber segmentation and introduced relevant metrics for a deeper understanding of the dermal matrix state. Eliminating the need for invasive sampling such as histology, this approach represents a significant advance toward in vivo monitoring of skin aging. In addition, prior work using OCT and LC-OCT have confirmed the potential of these imaging modalities for assessing dermal fiber structure; however, they were largely limited to qualitative observations or two-dimensional segmentation without quantitative analysis[35,54]. Multiphoton microscopy (MPM) with second-harmonic generation (SHG) and two-photon fluorescence (TPF) imaging, as reported by Wang et al.[54], allows simultaneous visualization of collagen and elastin fibers and provides excellent qualitative differentiation. These methods have consistently shown age- and photoaging-related changes in the dermal matrix, including reduced fiber density, shortened length, and loss of anisotropy with age. However, MPM remains confined to two-dimensional imaging and cannot deliver comprehensive volumetric data. While fluorescence-based methods are useful, they do not provide detailed information about the organization of the dermal fiber network. In contrast the combination of LC-OCT and dermal fiber characterization provides a powerful tool to gain a deeper understanding of the impact of age and ethnicity on dermal fibers, and how anti-aging skincare products influence the structural properties of dermal fibers. The results demonstrated that skin aging is associated with fiber fragmentation and a more anisotropic fiber network. Asians have a denser fiber network than Caucasians, with fibers more numerous and more reticulated. The cosmetic routine products applied daily to the face induced an increase in fiber synthesis and the creation of new connections between fibers and a more isotropic fiber network, as highlighted in this study's schematic illustration of dermal fiber response after one month of cosmetic treatment.

By integrating advanced LC-OCT imaging with a robust, fully automated 3D segmentation pipeline, this work represents a significant technological breakthrough. It provides a first-time level of detail in the in vivo characterization of dermal fibers, establishing a new paradigm for dermatological research. As the first study to apply this approach, our findings lay the foundation for future investigations into skin aging, ethnicity-driven differences, and the efficacy of skincare formulations, opening new perspectives for fundamental research in dermatology and cosmetic applications.

Methods

Clinical studies

Two clinical studies were conducted as part of this research.

The common inclusions criteria for both studies were, women with a phototype I to IV according Fitzpatrick scale, normal to dry face skin, subject not frequently user of cosmetic products (having a routine with 2 or 3 at most). Women were excluded from the study if they had recent sun exposure (natural or artificial) or had applied self-tanner or a tanning activator (dietary supplement) on the face within 4 weeks prior to inclusion. Additional exclusion criteria included visible irritation, hair, scars, tattoos, veins, or pigmentary spots on the study areas (face) that could interfere with evaluations or measurements, as well as the use of any facial products on the day of inclusion (water only permitted). Pregnancy or breastfeeding women were not included.

The first study aimed to assess skin aging and compare Caucasian to Asian women.

Two distinct age groups of volunteers were recruited. The first group consisted of 17 Asians and 16 Caucasians, aged between 20 and 30 years old. The second group comprised 10 Asians and 17 Caucasians, aged between 50 and 60 years old. The second study was an open, uncontrolled study, conducted to assess the efficacy of anti-aging products over a three-month period in 31 female Caucasian participants aged between 30 and 65 years old, presenting with a lack of firmness face skin, user of moisturizer product (not user of anti-wrinkles/firmness product, 4 weeks wash out). Subjects were asked to apply a serum and a cream on the whole face twice a day in normal conditions of use. The core active ingredient of the anti-aging product is botanical alfalfa concentrate. The first application was carried out at the investigational center under the control of the technical staff. Participants were instructed to not apply any skin products to their face on the mornings of the LC-OCT measurement days. These measurements were taken at three timepoints: t_0 (prior to the start of the care routine), t_1 (after one month) and t_3 (after three months).

The first study was conducted during the autumnal season, while the second study was conducted during the spring, in order to minimize any potential influence of solar radiation on the skin's properties.

Image acquisition

LC-OCT (DAMAE Medical, France, Paris) is a non-invasive imaging technique based on interferometry and low-coherence light principles. LC-OCT generates high-resolution cross-sectional images of biological tissues, horizontal images and 3D stacks. The device produces vertical and horizontal sectional images at a rate of eight frames per second, with a depth penetration of approximately 500 µm. LC-OCT has an axial resolution of 1.1 µm, a lateral resolution of 1.3 µm, and a field of view of 1.2 mm×0.5 mm (vertical) and 1.2 mm×0.5 mm (horizontal). In conjunction with microscopic imaging, the device offers a color macroscopic imaging modality along with real-time localization of the imaged region, facilitating precise targeting of the area of interest. This macroscopic surface image encompasses a 2.5 mm diameter field of view with a resolution of approximately 5 µm[10,12,13,55,56].

In this study, the device was used to obtain high-resolution 3D images of the skin on cheekbone. The procedure for in vivo human skin acquisition involves the application of a drop of paraffin oil between the skin and the glass window of the handheld probe[10,12,13,55,56]. The resulting 3D stacks were processed using an in-house developed algorithm for dermal fiber segmentation and various metrics were calculated. This image processing algorithm is based on the evaluation of Hessian-based multiscale measurements and automated thresholding techniques. All imaging acquisitions were conducted at controlled room laboratory temperature, with the volunteers lying down on a medical chair to minimize motion artefacts during acquisition.

Image processing

Multiple image processing techniques were applied to the images in order to first extract the dermal fibers and then compute different metrics. LC-OCT images (Fig. 4A1) were grayscale images with dimensions 1200 × 1200 × 300 μm^3 for the first study and 1276 × 500 × 300 μm^3 for the second study. The images acquired in the two studies exhibit disparate dimensions due to the evolution of the system between them. However, this evolution affecting only the field of view, the scanning depth, resolution, spectral range and imaging modes remained unchanged to ensure data comparability. The dermis volume analyzed in the two clinical studies had a thickness of 40 µm and started at the dermal-epidermal junction (Fig. 4B). The first step of the image processing (Fig. 4C) involved the enhancement of µm corresponding to dermal fibers via a methodology based on generic multiscale Hessian-based measures[57], which represents a generalization of Frangi's vesselness measure. Given that the pixel size is 1 µm, the spatial resolution for the image stacks is therefore 1 µm/pixel in all dimensions. This approach is a well-known technique in the medical field for enhancing blood vessels visualization in an image. The approach also allowed to extract the direction for each µm's enhanced structures by computing the eigenvectors of their Hessian matrix which describe the principal directions of curvature. The second step involved the segmentation of fibers on the enhanced image. This was achieved by applying an automated threshold that separated the µm into foreground (fibers) and background classes. Various thresholding methods were provided[58] to use the best non-biased approach preserving the fibers network for each image in the study. To be less sensitive to the threshold value which has influence on the thickness of the fibers network, the third step involved the extraction of the centerline of fibers (Fig. 4D) by using a binary thinning algorithm[59], which reduced each shape to a one-µm-wide line. The final step involved the computation of metrics based on the centerline of fibers.

In order to compute the numbers of nodes, mean length and number of fibers, it was first necessary to identify the points in the centerline that corresponded to nodes in the fibers network. This was accomplished by iterating through all the points in the centerline and identifying those having more than two neighbors (Fig. 5A). The total of these points gave the number of nodes. The fibers were then counted by removing the node points and computing the number of connected components, and their mean length was measured based on the number of points in each connected component. The length refers to the distance between the first and last points of each identified fiber's centerline within the 3D volume. Furthermore, two distinct fiber classes were identified. Connected fibers were defined as having at least one node, while isolated fibers lack nodes and appear as isolated components. The fiber network density (Df) was calculated by multiplying the number of fibers (Nf) by their mean length (and dividing by the total number (N) of pixels in the dermis volume (Df = Nf × Lm/N of pixels).

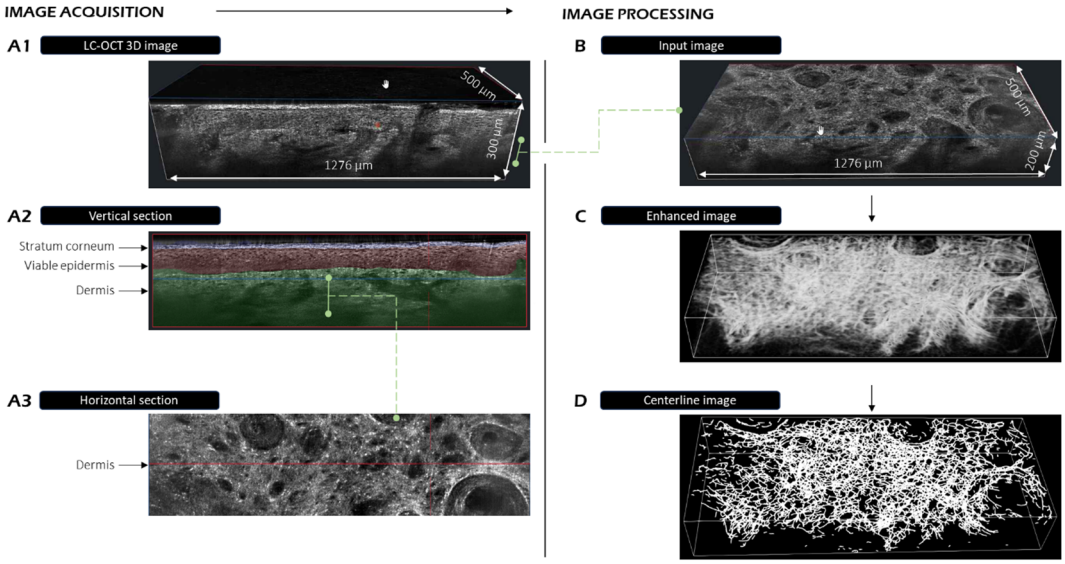

Fig. 4. LC-OCT images of human skin in vivo, highlighting the key features of the images (**A1**,**A2**,**A3**) and the main steps of the image processing (**B**–**D**). (**A1**) 3D stack of skin. (**A2**) 2D vertical image with labels for the different skin layers. (**A3**) 2D horizontal image of the dermis. (**B**) 3D stack of the analyzed dermis volume, starting at the dermal-epidermal junction with a thickness of 200 µm (the first 40 µm were retained for analysis). (**C**) 3D segmentation of dermal fibers using Frangi's algorithm. (**D**) Extraction of fiber centerlines using a binary thinning algorithm.

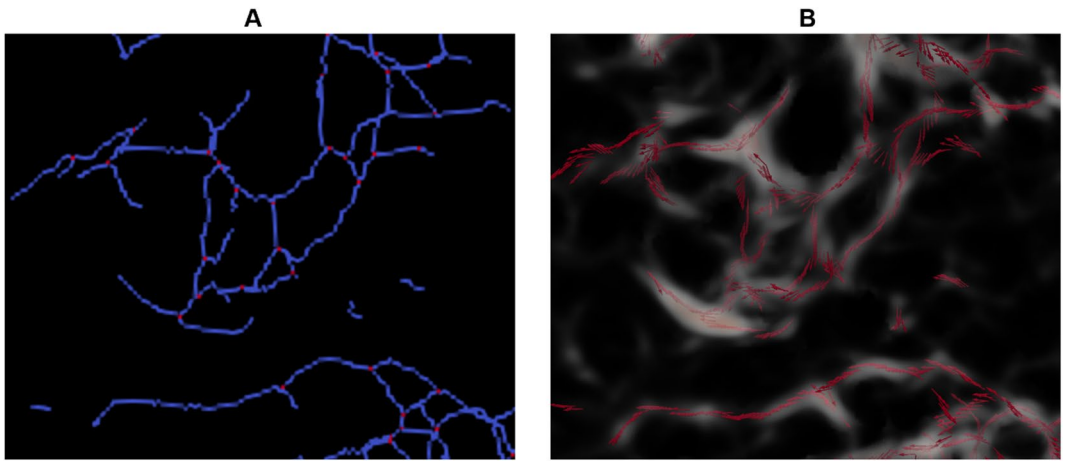

Fig. 5. Centerline nodes points (**A**) and computed directions on the enhanced image (**B**).

The anisotropy score, which is a measure of the irregularity of fiber orientation in the dermis, was calculated by analyzing the sum of the direction matrices (generated in the first step, Fig. 5B).

The score was computed from the ratio of the eigenvalues of the resulting direction matrix. Eigenvalues being similar means that the direction vectors are equally distributed, while having larger eigenvalues than others highlight a predominant direction. When the score is equal to zero, the fibers have a pluri-directional organization, and when it is equal to 1, the fibers have a unidirectional organization.

Statistical analysis

Statistical analyses have been run on R (version 4.2.2). For study 1, to determine whether there was a significant effect of the age factor (young vs. aged), ethnicity factor (Caucasian vs. Asian) and possible interaction age x ethnicity on dermal fiber characteristics (numbers, mean length, nodes, density and anisotropy score), a two-ways ANOVA was performed. When the interaction was not significant, the interaction was removed from the model. The assumption of normal distribution of residuals was tested using Shapiro-Wilk test and graphically (Quantile-Quantile plot). For all metrics, the assumption of normality of residuals was not rejected, and no significant interaction age x ethnicity was highlighted. For study 2, to determine whether there was a significant change in the characteristics of the dermal fibers after skin care products application, mean comparison tests

for paired data have been carried out between the baseline T0 and T1, and the baseline T0 and T3. First, the both differences were calculated: T1 – T0, and, T3 – T0. Then, a Paired t-test was applied when the data were normally distributed, otherwise a Wilcoxon signed rank test was applied. The assumption of normal distribution was tested using Shapiro-Wilk test and graphically (Quantile-Quantile plot). Graphical visualizations (boxplots) have been produced to illustrate the analysis of the results.

Data availability

The data that support the findings of this study are available from the corresponding author upon reasonable request.

Received: 1 July 2025; Accepted: 29 September 2025
Published online: 04 November 2025

References

1. Mukae, S., Ogura, Y. & Hara, Y. Characterization of the collagen network of human cheek skin using ultrasonic microscopy. *Ultrasonics* **139**, 107299 (2024).
2. Witt, N. J., Woessner, A. E., Herrmann, J., Quinn, K. P. & Sander, E. A. Mechanical models of collagen networks for Understanding changes in the failure properties of aging skin. *J. Biomech. Eng.* **146**, 071002 (2024).
3. Le Digabel, J., Houriez-Gombaud-Saintonge, S., Filiol, J., Lauze, C. & Josse, G. Dermal fiber structures and Photoaging. *J. Biomed. Opt.* **23**, 1 (2018).
4. Shin, S. H., Lee, Y. H., Rho, N. K. & Park, K. Y. Skin aging from mechanisms to interventions: focusing on dermal aging. *Front. Physiol.* **14**, 1195272 (2023).
5. Chekanov, K. et al. State-of-the-Art in skin fluorescent photography for cosmetic and skincare research: from molecular spectra to AI image analysis. *Life* **14**, 1271 (2024).
6. Goberdhan, L. T. et al. Assessing changes in facial skin quality using noninvasive in vivo clinical skin imaging techniques after use of a topical retinoid product in subjects with moderate-to-severe photodamage. *Skin. Res. Technol.* **28**, 604–613 (2022).
7. Babalola, O., Mamalis, A., Lev-Tov, H. & Jagdeo, J. Optical coherence tomography (OCT) of collagen in normal skin and skin fibrosis. *Arch. Dermatol. Res.* **306**, 1–9 (2014).
8. Lentsch, G. et al. Research techniques made simple: emerging imaging technologies for noninvasive optical biopsy of human skin. *J. Invest. Dermatology*. **142**, 1243–1252e1 (2022).
9. Dubois, A., Siret, D. & Barut, A. L'imagerie de La peau par LC-OCT. *Photoniques* 36–39. https://doi.org/10.1051/photon/202312336 (2023).
10. Dubois, A. et al. Line-field confocal optical coherence tomography for high-resolution noninvasive imaging of skin tumors. *J. Biomed. Opt.* **23**, 1 (2018).
11. Pedrazzani, M. et al. Comparison of line-field confocal optical coherence tomography images with histological sections: validation of a new method for in vivo and non-invasive quantification of superficial dermis thickness. *Skin. Res. Technol.* **26**, 398–404 (2020).
12. Chauvel-Picard, J. et al. Line-field confocal optical coherence tomography as a tool for three-dimensional in vivo quantification of healthy epidermis: A pilot study. *J. Biophotonics*. **15**, e202100236 (2022).
13. Ogien, J., Levecq, O., Azimani, H. & Dubois, A. Dual-mode line-field confocal optical coherence tomography for ultrahigh-resolution vertical and horizontal section imaging of human skin in vivo. *Biomed. Opt. Express*. **11**, 1327 (2020).
14. Reihsner, R., Balogh, B. & Menzel, E. J. Two-dimensional elastic properties of human skin in terms of an incremental model at the in vivo configuration. *Med. Eng. Phys.* **17**, 304–313 (1995).
15. Zhou, M. et al. Three-dimensional Characterization of Mechanical Properties and Microstructures of Human Dermal Skin. Preprint at (2023). https://doi.org/10.21203/rs.3.rs-3303648/v1.
16. Shin, J. W. et al. Molecular mechanisms of dermal aging and antiaging approaches. *IJMS* **20**, 2126 (2019).
17. Quan, T. & Fisher, G. J. Role of Age-Associated alterations of the dermal extracellular matrix microenvironment in human skin aging: A Mini-Review. *Gerontology* **61**, 427–434 (2015).
18. Nguyen, T. T. et al. Changes of skin collagen orientation associated with chronological aging as probed by polarized-FTIR micro-imaging. *Analyst* **139**, 2482 (2014).
19. Rittie, L. & Fisher, G. J. Natural and Sun-Induced aging of human skin. *Cold Spring Harbor Perspect. Med.* **5**, a015370–a015370 (2015).
20. He, T., Fisher, G. J., Kim, A. J. & Quan, T. Age-related changes in dermal collagen physical properties in human skin. *PLoS ONE*. **18**, e0292791 (2023).
21. Ma, W. et al. Chronological ageing and Photoageing of the fibroblasts and the dermal connective tissue: ageing of fibroblasts and connective tissue. *Clin. Exp. Dermatol.* **26**, 592–599 (2001).
22. Arnal-Forné, M. et al. Changes in human skin composition due to intrinsic aging: a histologic and morphometric study. *Histochem. Cell. Biol.* **162**, 259–271 (2024).
23. Ali, A. et al. Comparison of facial skin ageing in healthy Asian and Caucasian females quantified by in vivo line-field confocal optical coherence tomography 3D imaging. *Skin. Res. Technol.* **30**, e13643 (2024).
24. Lin, K., Liao, Y., Wei, M. & Sun, C. Comparative analysis of intrinsic skin aging between Caucasian and Asian subjects by slide-free in vivo harmonic generation microscopy. *J. Biophotonics*. **13**, e201960063 (2020).
25. Ling, L. C. Aging in Asian Skin. in *Textbook of Aging Skin* (eds. Farage, M. A., Miller, K. W. & Maibach, H. I.) 1019–1024Springer Berlin Heidelberg, Berlin, Heidelberg, (2010). https://doi.org/10.1007/978-3-540-89656-2_94
26. Rawlings, A. V. Ethnic skin types: are there differences in skin structure and function?[1]. *Intern. J. Cosmet. Sci.* **28**, 79–93 (2006).
27. Vashi, N. A. *Aging Differences Ethnic Skin*. **9**, (2016).
28. Griffiths, T. W., Watson, R. E. B. & Langton, A. K. Skin ageing and topical rejuvenation strategies. *Br. J. Dermatol.* **189**, i17–i23 (2023).
29. Monnier, J. et al. In vivo characterization of healthy human skin with a novel, non-invasive imaging technique: line-field confocal optical coherence tomography. *Acad. Dermatol. Venereol.* **34**, 2914–2921 (2020).
30. Del Río-Sancho, S., Gallay, C., Ventéjou, S. & Christen-Zaech, S. In vivo evaluation of skin of children with LC-OCT: an objective assessment. *Acad. Dermatol. Venereol.* **37**, 1897–1905 (2023).
31. Jdid, R. et al. Skin dark spot mapping and evaluation of brightening product efficacy using Line-field confocal optical coherence tomography (LC-OCT). *Skin. Res. Technol.* **30**, e13623 (2024).
32. Bonnier, F. et al. Line-field confocal optical coherence tomography coupled with artificial intelligence algorithms to identify quantitative biomarkers of facial skin ageing. *Sci. Rep.* **13**, 13881 (2023).
33. Razi, S., Raquepo, T. M., Truong, T. M. & Rao, B. Analyzing the effects of a chemical Peel on post-inflammatory hyperpigmentation using line-field confocal optical coherence tomography. *Skin. Res. Technol.* **29**, e13496 (2023).
34. Fischman, S. et al. Non-invasive scoring of cellular atypia in keratinocyte cancers in 3D LC-OCT images using deep learning. *Sci. Rep.* **12**, 481 (2022).

35. Ayadh, M. et al. LC-OCT Imaging for Studying the Variation of Morphological Properties of Human Skin In Vivo According to Age and Body area: The Forearm and the Thigh. *neo.* 2, (2022).
36. Baumann, L. et al. Clinical relevance of Elastin in the structure and function of skin. *Aesthetic Surg. J. Open. Forum*. **3**, ojab019 (2021).
37. Lynch, B. et al. A mechanistic view on the aging human skin through ex vivo layer-by-layer analysis of mechanics and microstructure of facial and mammary dermis. *Sci. Rep.* **12**, 849 (2022).
38. Blair, M. J., Jones, J. D., Woessner, A. E. & Quinn, K. P. Skin Structure–Function relationships and the wound healing response to intrinsic aging. *Adv. Wound Care*. **9**, 127–143 (2020).
39. Fligiel, S. E. G. et al. Collagen degradation in Aged/Photodamaged skin in vivo and after exposure to matrix Metalloproteinase-1 in vitro. *J. Invest. Dermatology*. **120**, 842–848 (2003).
40. Qin, Z., Balimunkwe, R. M. & Quan, T. Age-related reduction of dermal fibroblast size upregulates multiple matrix metalloproteinases as observed in aged human skin *in vivo*. *Br. J. Dermatol.* **177**, 1337–1348 (2017).
41. Marcos-Garcés, V. et al. Age-related dermal collagen changes during development, maturation and ageing – a morphometric and comparative study. *J. Anat.* **225**, 98–108 (2014).
42. Eklouh-Molinier, C. et al. Investigating the relationship between changes in collagen fiber orientation during skin aging and collagen/water interactions by polarized-FTIR microimaging. *Analyst* **140**, 6260–6268 (2015).
43. Ahmed, T. et al. Combining nano-physical and computational investigations to understand the nature of aging in dermal collagen. *IJN* **12**, 3303–3314 (2017).
44. Yasui, T., Takahashi, Y. & Araki, T. Polarization-resolved second-harmonic-generation imaging of photoaged dermal collagen fiber. in (eds. Periasamy, A. & So, P. T. C.) 71831XSan Jose, CA, (2009). https://doi.org/10.1117/12.808672.
45. Fukushima, S. Polarization-resolved second-harmonic-generation imaging of dermal collagen fiber in prewrinkled and wrinkled skins of ultraviolet-B-exposed mouse. *J. Biomed. Opt.* **24**, 1 (2018).
46. Richards, G. M., Oresajo, C. O. & Halder, R. M. Structure and function of ethnic skin and hair. *Dermatol. Clin.* **21**, 595–600 (2003).
47. Von Stebut, E. & Helbig, D. Anatomische und funktionelle unterschiede der Haut verschiedener ethnien. *Dermatologie* **74**, 80–83 (2023).
48. Fantasia, J. et al. Differential levels of Elastin fibers and TGF-β signaling in the skin of Caucasians and African Americans. *J. Dermatol. Sci.* **70**, 159–165 (2013).
49. Girardeau, S., Mine, S., Pageon, H. & Asselineau, D. The Caucasian and African skin types differ morphologically and functionally in their dermal component. *Exp. Dermatol.* **18**, 704–711 (2009).
50. Quan, T. Human skin aging and the Anti-Aging properties of retinol. *Biomolecules* **13**, 1614 (2023).
51. Rossetti, D. et al. A novel anti-ageing mechanism for retinol: induction of dermal Elastin synthesis and Elastin fibre formation. *Intern. J. Cosmet. Sci.* **33**, 62–69 (2011).
52. Zasada, M. & Budzisz, E. Retinoids: active molecules influencing skin structure formation in cosmetic and dermatological treatments. *Pdia* **36**, 392–397 (2019).
53. Humbert, P. G. et al. Topical ascorbic acid on photoaged skin. Clinical, topographical and ultrastructural evaluation: double-blind study vs. placebo. *Exp. Dermatol.* **12**, 237–244 (2003).
54. Wang, H., Shyr, T., Fevola, M. J., Cula, G. O. & Stamatas, G. N. Age-related morphological changes of the dermal matrix in human skin documented in vivo by multiphoton microscopy. *J. Biomed. Opt.* **23**, 1 (2018).
55. Ogien, J., Daures, A., Cazalas, M., Perrot, J. L. & Dubois, A. Line-field confocal optical coherence tomography for three-dimensional skin imaging. *Front. Optoelectron.* **13**, 381–392 (2020).
56. Dubois, A. et al. Line-field confocal time-domain optical coherence tomography with dynamic focusing. *Opt. Express*. **26**, 33534 (2018).
57. Antiga, L. Generalizing vesselness with respect to dimensionality and shape. *Insight J.* https://doi.org/10.54294/urgadx (2007).
58. Huang, C., Li, X. & Wen, Y. AN OTSU image segmentation based on fruitfly optimization algorithm. *Alexandria Eng. J.* **60**, 183–188 (2021).
59. Homann, H. Implementation of a 3D thinning algorithm. *Insight J.* https://doi.org/10.54294/xjdr5f (2007).
60. WMA - The World Medical Association-WMA Declaration of Helsinki – Ethical Principles for Medical Research. Involving Human Participants. https://www.wma.net/policies-post/wma-declaration-of-helsinki/.

Acknowledgements

We gratefully acknowledge the DAMAE group for providing access to the LC-OCT measurement device.

Author contributions

K.K. researcher who conducted , authored this study and wrote the main manuscript text ; R.J. Investigator of the study and contributed to the drafting of the paper; J.L. and O.T. Data collection and analysis; K.K., G.C. and L.G. development of algorithms for dermal fibers segmentation and characterization; S.P.: data acquisition; J.L., NA, G.C. and Y.B.K. results validation and manuscript review. All authors reviewed and approved of the final manuscript.

Declarations

Competing interests

Chanel employees (Kamilia Kemel, Randa Jdid, Julie Latreille, Nada André, Gabriel Cazorla, Youcef Ben Khalifa) have no conflicts of interest to declare. Oriane Tarby is employee of IT&M Stat, which was funded by Chanel for data analyses. Lucas Gandel is employee of Kitware Europe, was funded by Chanel to develop the algorithms. Severine Ponsero is employee of DERMATECH, was funded by Chanel for data acquisition.

Ethics statement

The two clinical studies were conducted in accordance with the Declaration of Helsinki[60]. All participants provided written informed consent and a photo consent statement before starting the study. This research is exempted from an Ethic Committee approval according to the French Public health code, research involving human participants, articles L1121-1 to L1128-12 (https://www.legifrance.gouv.fr).

Additional information

Supplementary Information The online version contains supplementary material available at https://doi.org/1

0.1038/s41598-025-22349-9.

Correspondence and requests for materials should be addressed to K.K.